Nature of the metastable boron–oxygen complex formation in crystalline silicon

Richard S. Crandall[a)]
National Renewable Energy Laboratory, Golden Colorado 80401, USA

(Received 7 May 2010; accepted 20 August 2010; published online 23 November 2010)

Transient capacitance measurements reveal new physics of metastable defect formation in boron-doped oxygen-containing crystalline silicon solar cells. These measurements demonstrate that holes are deeply trapped during defect formation and removed during thermal annealing with activation energy of 1.3 eV. Previous theoretical models {Du *et al.*, [Phys. Rev. Lett. **97**, 256602 (2006)] and Adey *et al.*, [Phys. Rev. Lett. **93**, 055504 (2004)]} are supported by present findings that defect formation is a slow two-stage process with activation energies of 0.17 eV and 0.4 eV at high and low temperature, respectively. Repulsive hole capture by a positive oxygen-dimer determines the defect formation rate at low temperature {Du *et al.*, [Phys. Rev. Lett. **97**, 256602 (2006)]}. The high temperature process is governed by a structural conversion of the dimer {Du *et al.*, [Phys. Rev. Lett. **97**, 256602 (2006)] and Adey *et al.*, [Phys. Rev. Lett. **93**, 055504 (2004)]}. An abnormally low rate prefactor allows this low-enthalpy reaction to be observed at the higher temperature. This dimer conversion presents an excellent example of an "entropy barrier" that explains the low conversion rate. Disparate formation and annealing results published here and in other publications are related by the Meyer–Neldel rule with an isokinetic temperature of 410 K. © *2010 American Institute of Physics*. [doi:10.1063/1.3490754]

I. INTRODUCTION

The metastable defect-producing light-induced degradation in boron-doped Czochralski (Cz)-Si is a fascinating scientific and important technological problem. Experiments[1–6] show that only if B and O are both present, will prolonged illumination reduce the minority carrier lifetime. A quadratic correlation of the relative number of defects per B atom with the oxygen concentration led Schmidt, Bothe, and Hezel to postulate that the defect is a BO_2 complex.[3] Crystalline solar cells made from B-doped Cz-Si lose as much as 10% of their efficiency during operation due to light-induced defects. This is a serious problem for the widespread use of these low cost wafers for photovoltaic applications. One must either use float-zone (FZ) silicon or another dopant, both of which are costly for the industry.

A number of experiments have yielded salient information about the defect responsible for solar cell degradation.[3–15] Defects can be formed by; illumination of a wafer of c-Si,[3–10,15] a solar cell,[11,12,14] or by forward biasing a solar cell in the dark.[13] The relative degradation has been probed by either a reduction in the minority carrier lifetime or a reduction in open-circuit voltage. Early photoconductivity measurements indicated that the energy level for recombination associated with the defect is located about midgap.[8,9] More recent measurements using advanced lifetime spectroscopy place the level 0.41 eV below the conduction band, E_c.[10]

Fortunately the rate of degradation is slow. At low light intensity it varies linearly with intensity[4] because minority carrier electrons[1] limit the degradation rate. The degradation rate saturates at high intensity[4] where hole capture[1] is the rate-limiting step. The thermal activation energy, E_a, for light-induced defect production is about 0.4 eV.[3,11,14,15] The defect is metastable requiring high temperature, T, to remove it. Values of thermal activation energy for annealing have been reported ranging from 1.3 to 1.8 eV.[3,4,11]

Following the suggestion[3,4] that the defect was formed by the migration of oxygen dimers to B atoms, Adey *et al.*[2] presented a theory describing the dynamics of dimer migration. They proposed that the dimer possesses two distinct structures; square (SQ) and staggered (ST). By trapping and emitting an electron, the dimer can flip between these two structures. Therefore, under illumination or minority carrier injection the dimer is able to diffuse. The predicted equilibrium state of the SQ structure in p-type Si is $O_2^{sq,++}$. The proposed diffusion mechanism is $O_2^{sq,++} \rightarrow O_2^{st,+} \rightarrow O_2^{sq,++}$ with activation energy of 0.3 eV.[2] In this manner, the dimer diffuses until it meets a B_4^- and becomes bound to it by Coulomb attraction. The resulting defect could be either negative or positive depending on the dimer structure and charge. However, the preferred structure would most likely be the $BO_2^{sq,+}$ because of the strong attraction between B_4^- and $O_2^{sq,++}$. The calculations of Adey *et al.*[2] were refined by Du *et al.*[1] who differ on the ground state configuration and point out that the dimer energy levels are nearly unchanged by the proximity of the B_4^-. Du *et al.*[1] present new understanding of the mechanism of recombination at the BO_2 complex and the details of the dimer diffusion.

Adey *et al.*[2] place the 0/+ level of the defect at about 0.2 eV below E_c. Du *et al.*[1] also place this level close to the conduction band. However, this is only true if the level is empty. Once it captures an electron, strong lattice relaxation moves this level close to the valence band as the dimer re-

a)Electronic mail: bellucci@lnf.infn.it.

configures from SQ to ST structure.[1] The level remains there until the dimer captures a hole and reconfigures back to the ST structure. This cyclic recombination is also present when the dimer is bound to the boron atom.

The purpose of this manuscript is to measure the charge change upon defect formation or removal using transient capacitance techniques. The details of dimer diffusion involve charge change at each step.[1,2] Prior experiments measured only a change in electron-hole recombination upon defect formation and thus did not probe details of defect formation which can be probed by capacitance transients that measure charge change. Section II describes the details of sample preparation and measurement technique. This section also presents both defect formation measurements in part A and defect annealing in part B. Section III discusses these results in terms of theory and compares them with earlier work. I explain the slow reaction rates for defect formation by an "entropy barrier." Results are summarized in Sec. IV.

II. EXPERIMENT

To determine the charge change during metastable defect formation, I apply junction-capacitance methods[16] using a lock-in amplifier (Stanford Instruments Model 850) at a frequency of 100 kHz and an ac test voltage of 0.03 V rms. The sample is placed in a holder capable of maintaining a stable temperature (± 0.1 K) between 100 and 600 K. A high power light-emitting diode (LED) (840 nm) illuminates the sample with an intensity of about 5 mW cm^{-2}. This intensity is high enough to satisfy the condition that the defect formation rate depends on holes rather than electrons.[1,4] Samples are two Cz and one FZ B-doped Si solar cells with doping of 3, 13, and 66×10^{15} cm^{-3}, respectively. The FZ sample uses a P-doped diffused junction and contains 9×10^{18} cm^{-3} oxygen as determined by secondary ion mass spectroscopy. The 2CZ-Si samples are fabricated with an amorphous silicon heterojunction emitter.[17]

A. Charge trapping

The following three step experiment determines the charge change and rate of metastable defect formation. (1) Reverse bias the sample and measure the capacitance, C_0. (2) Switch the bias to 0 V or a small forward bias and illuminate the sample for a short time. (3) Turn off the light and return to reverse bias to measure the capacitance. This capacitance measurement takes about 1 s. This procedure continues until defects are formed as indicated by a capacitance change, ΔC. The sign of ΔC indicates the type of charge that is trapped; negative for majority (holes) and positive for minority carriers. For more details on using transient capacitance measurements to probe metastable defect formation and annealing, see Ref. 16.

During step (2) it is necessary to collapse the depletion region to trap charge and form defects. If the device remains at reverse bias there is no charge change, even under prolonged illumination. The reason for this can be seen with the aid of Fig. 1 that shows the free hole density versus distance in the region of the n/p junction. At reverse bias the depletion region is virtually devoid of holes except near the edge of the

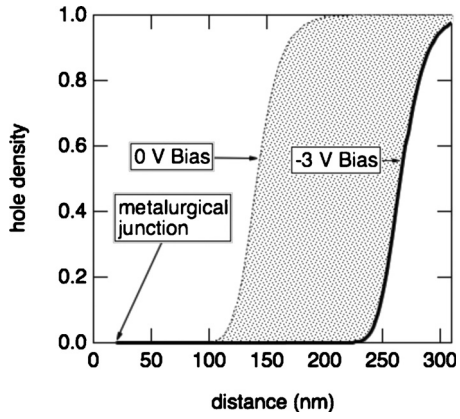

FIG. 1. Charge density diagram that shows how the hole density changes with bias change. The top of the cell is at 0 nm. The density is normalized to the bulk value of holes.

depletion region (300 nm) where some holes diffuse in from the bulk. Under illumination electrons are swept to the junction region and holes are swept into the bulk in less then 1 μs, much less than the time required to form defects. Of course there are photogenerated electrons in the bulk that can form defects there. However, capacitance is insensitive to these because of charge neutrality requirements. At forward or 0 bias the bulk density of holes extends well into the reverse bias depleted region as shown by the dotted region in Fig. 1. In addition this region is now field-free so that photogenerated electrons remain near holes long enough to form defects.

Figure 2 shows a capacitance transient at 323 K during illumination. Beginning around 10 s, ΔC decreases indicating hole trapping. As I show in Sec. II B, holes are deeply trapped indicating metastable defect formation. The solid line is an exponential fit to the fractional capacitance change. Repeating this procedure to determine the reaction rate, $\mathbf{r_c}$, at different temperatures allows one to find the activation energy and rate prefactor, υ_c, for defect formation from an Arrhenius plot.

Figure 3 is an Arrhenius plot of the hole trapping rate versus reciprocal temperature. The slope of the lines in the figure determines the activation energy in the usual way. The

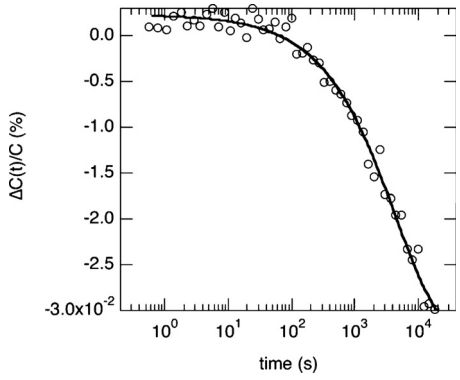

FIG. 2. Relative capacitance change vs illumination time at 333 K for a Cz solar cell containing 1.3×10^{16} cm^{-3} boron. The bias is -1 V for measurement and 0 V during LED illumination. The line is $\Delta C(t)/C = Ae^{-r_c t}$ where t is the measuring time and r_c the characteristic annealing rate. $r_c = 0.000\,54$ s^{-1}.

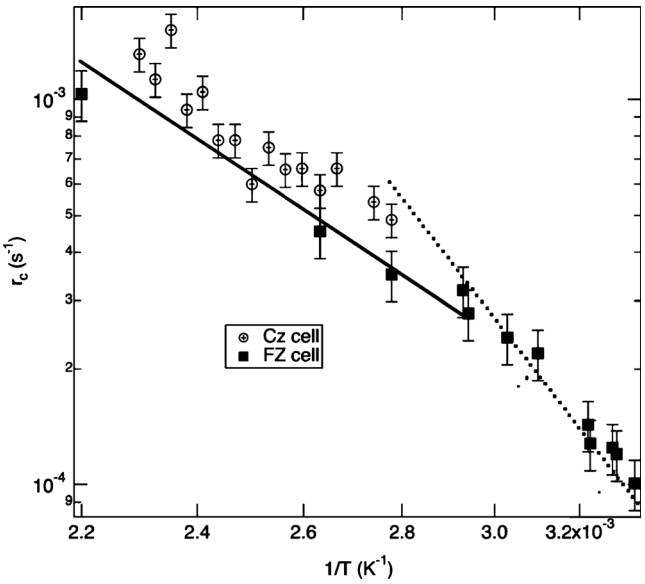

FIG. 3. An Arrhenius plot of the characteristic degradation rate under illumination. The parameters for the solid line are E_a=0.17 eV and υ_c =0.1 s^{-1}. The parameters for the dotted line are E_a=0.4 eV and υ_c =293 s^{-1}. The Cz cell contains 1.3×10^{16} cm^{-3} boron and the FZ cell 6.6×10^{16} cm^{-3} boron.

dotted line represents activation energy of 0.4 eV. The low temperature data fall along this line. However, above about 330 K the data fall along the solid line with a slope of 0.17 eV. The low temperature measurements give the same activation energy and nearly the same prefactor as determined by others using photocarrier lifetime or open-circuit voltage reduction to determine the degradation rate at low temperature.[3,4,11,15]

At high temperature a process with low activation energy and an abnormally low rate prefactor, υ_c=0.1 s^{-1}, is the limiting reaction. At low temperature another process with a higher activation energy and higher rate prefactor, υ_c =293 s^{-1}, dominates the overall defect formation. In any series multistep-process the rate-limiting step is always the one which is slowest at the measuring temperature. I will discuss the nature of these processes in Sec. III.

B. Charge emission

The following three step procedure measures trapped hole emission to determine the annealing kinetics of the metastable defect. (1) Heat the sample to about 500 K at reverse bias for about 5 min to anneal out any residual defects in the depletion region. Cool the sample, while holding at reverse bias, to the measurement temperature and record the capacitance. (2) Increase the bias to forward bias and illuminate the sample for about 1000 s to inject electrons and holes and form metastable defects as described above. (3) At the end of this time, extinguish the light and switch to reverse bias. Measure capacitance as a function of time, t, until all the trapped charge has left the device and the capacitance returns to its baseline value.

Figure 4 shows an annealing transient at 410 K taken during step (3). ΔC, initially large and negative, begins to increase at about 1 s as the defects anneal and holes are

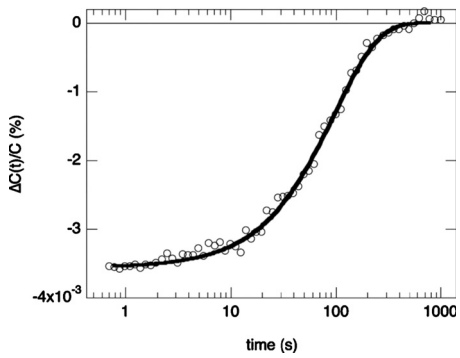

FIG. 4. Relative capacitance change vs annealing time measured at 410 K on a Cz solar cell containing 1.3×10^{16} cm^{-3} boron. The bias is −1 V for measurement and 0 V during a 1000 s LED illumination.

emitted. Any free holes are swept out during the initial part of the transient at times too short to measure. At about 600 s all trapped holes are emitted and swept from the depletion region and the capacitance returns to the value before defect formation.

Repeating this procedure to determine the annealing rate at different temperatures allows one to find the defect annealing energy from an Arrhenius plot. Figure 5 shows the annealing rate versus reciprocal temperature. The slope of the plot determines a thermal activation energy of E_a =1.33 ± 0.05 eV and rate prefactor, $\upsilon_c=2.6\times10^{14}s^{-1}$.

Since both annealing and degradation activation energies are similar to values found by others, it seems clear that the metastable defect measured here by capacitance is the same as that probed by minority carrier lifetime measurements. Defect formation and annealing activation energies values from this study as well as literature values are plotted in Fig. 6.

III. DISCUSSION

A. Defect formation

The method used to measure the charge trapping rate determines to some extent what can be observed. Experiments carried out in the bulk such as those discussed in the introduction begin with the dimer in the $O_2^{sq,++}$ configuration because the Fermi level is close to the valence band.[1,2] Charge trapping experiments begin with the dimer in the

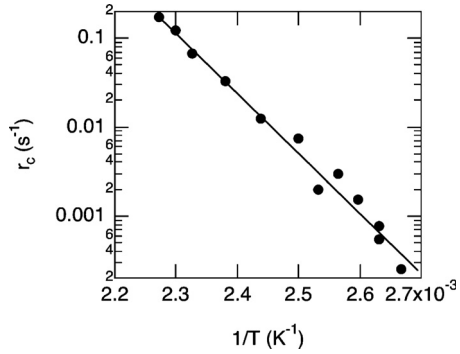

FIG. 5. Arrhenius plot of the characteristic annealing time for the device used for Fig. 4. Circles are measured values and the line is a fit to the data giving E_a=1.33 ± 0.05 eV and $\upsilon_c=2.6\times10^{14}$ s^{-1}.

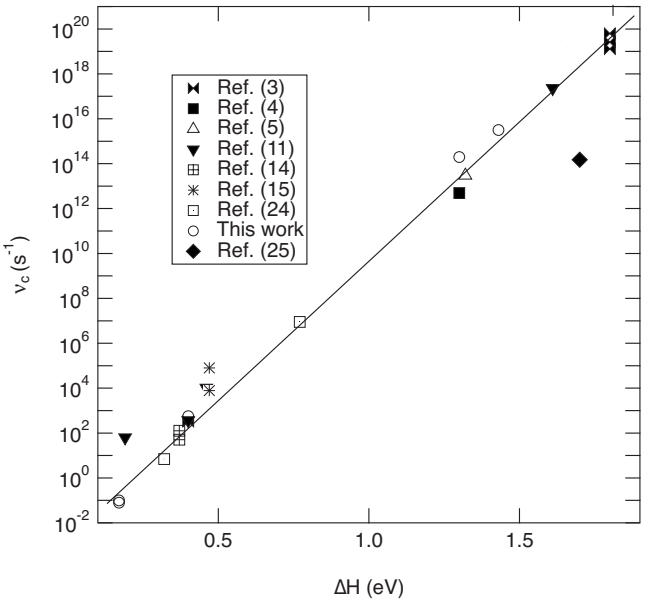

FIG. 6. Meyer–Neldel plot of rate prefactor vs activation energy. Data are from this work as well as from the literature. Data for annealing as well as degradation are shown on the plot.

depletion region where the high Fermi level ensures that it is neutral in the ST configuration.[1] Once the depletion width collapses, the following hole trapping reactions are possible:

(a) $O_2^{st,0} + h \rightarrow O_2^{st,+}$,

(b) $O_2^{st,+} + h \rightarrow O_2^{st,++}$,

(c) $O_2^{st,++} \rightarrow O_2^{sq,++}$.

The hole trapped in reaction (a) is not stable and is easily emitted. Once the second hole is trapped over the high repulsive Coulomb barrier in step (b), the final reconfiguration (c) must take place to move the holes close to the conduction band.[1] The dimer can then either remain in the $O_2^{sq,++}$ configuration or undergo light-induced migration.[1,2] If the dimer did not undergo migration and eventual BO_2 defect formation, the deeply trapped holes in (c) would be bound by about 0.9 eV.[1] However, because the measured activation energy for hole emission is 1.3 eV, the dimer presumably migrates to form the BO_2 defect with a higher annealing energy. Two holes are trapped for each defect formed.

Light-induced migration follows the steps described by the following reactions from Ref. 1:

(1) $O_2^{sq,++} + e^- \rightarrow O_2^{sq,+}$,

(2) $O_2^{sq,+} \rightarrow O_2^{st,+}$(reconfiguration),

(R) $O_2^{st,+} \rightarrow O_2^{st,+}$(O rotation),

(3) $O_2^{st,+} + h^+ \rightarrow O_2^{st,++}$(slow),

(4) $O_2^{st,++} + e^- \rightarrow O_2^{sq,++}$(reconfiguration).

A dimer in the SQ configuration captures an electron (1) and then reconfigures (2) and (R) to the ST configuration. Finally, it captures a hole and reconfigures (3) and (4) back to the original SQ structure. These carrier trappings and structure reconfigurations continue until the dimer meets a B_4^- and the BO_2 defect forms.

In the Adey *et al.*[2] model, steps (1) and (2) are the same. Step (3) is a fast electron emission and step (4) presents a reconfiguration barrier of 0.3 eV. In contrast, the Du *et al.*[1] model suggests that the barrier occurs at step (3) because of the repulsive Coulomb potential for hole capture by the positive dimer. Palmer *et al.*[15] lend further support to this conjecture by showing that the rate of capture is governed by the hole density. Rose[18] estimated a Coulomb barrier of about 0.4 eV for charge capture by a defect with the same charge. Others find similar values.[19]

The charge trapping experiment described above shows two distinct regions (see Fig. 3) marked by different activation energies above and below about 330 K. The low temperature region in Fig. 3 is presumably determined by the repulsive capture of the second hole in step (3). The 0.4 eV barrier found here and by others represents this capture. Above 330 K the rate-limiting step could be the SQ to ST reconfigurations as represented by steps (1) and (2).

Both models[1,2] require electron capture and then reconfiguration from the SQ to the ST structures as the initial stages of dimer diffusion since the barrier for the $O_2^{sq,++} \rightarrow O_2^{st,++}$ reconfiguration is 0.86 eV.[1,2] The $O_2^{sq,+} \rightarrow O_2^{st,+}$ reconfiguration following electron trapping reduces this thermal barrier to between 0.2 eV (Ref. 2) and 0.17 eV.[1] This reconfiguration must take place in less than a nanosecond so that the electron can remain trapped during the reconfiguration. For example, at 400 K electron emission from a level at $E_c - 0.2$ eV takes 0.3 ns assuming an attempt-to-escape frequency of 10^{12} s^{-1}. The Du *et al.*[2] model postulates that the electron is deep trapped due to relaxation as the defect reconfigures from SQ to ST structures. This process would then keep the electron from being thermally emitted permitting reconfiguration. However, this reconfiguration must still be fast enough to keep the electron from escaping. This could well be the case, but then the observed defect production rate would be limited by the repulsive Coulomb capture in step (3) rather than the fast steps (1) and (2). In this case the high temperature values of r_c would follow the dotted line in Fig. 3.

However, the high temperature data show the lower activation energy of 0.17 eV, typical of reaction (2) rather than the 0.4 eV expected for repulsive capture. I will show in Sec. III C that the overall reaction is slow even when its separate parts are fast because the reaction represent an entropy barrier.[20]

A further argument showing that different mechanisms are operative in the high and low temperature regions is that Palmer *et al.*[15] show that the rate of defect formation at low temperature scales as the SQ of the boron concentration. Thus, if the same mechanism were to control the degradation at high temperature where data for the Cz and FZ overlap, the rate for the FZ sample should be about 25 times higher then for the Cz sample.

B. Defect annealing

Thermal annealing of the BO_2 defect is the reverse of the formation process in that it requires the dimer to diffuse away from the B_4^-.[2] Assuming the defect is $BO_2^{sq,+}$, the first diffusion step $O_2^{sq,++} \rightarrow O_2^{st,++}$ has the highest barrier. It must overcome the 0.86 eV (Ref. 2) SQ to ST conversion energy barrier plus the Coulomb binding energy of either 0.38 (Ref. 2) or 0.55 eV.[1] As the dimer diffuses away it presumably follows the steps (1) to (4) when annealing takes place in the bulk. However, if annealing takes place in the depletion width, then the relevant energies are the Coulomb binding energy and the 0.9 eV emission energy of the reaction $O_2^{sq,++} \rightarrow O_2^{st,++} + 2h$. In either case the annealing energies would be about the same. Experimental values for activation energy for annealing of the BO_2 complex ranging from 1.3 to 1.8 eV as measured here by capacitance transients and by others as shown in Fig. 6.

C. Entropy effects

Neither model[1,2] addresses the extremely low defect formation rate measured by capacitance at high temperature. One would normally expect a much higher rate with such a low activation energy of 0.17 eV. It is most likely that one of the steps in the dimer reconfiguration presents an entropy barrier.[20] Often one ignores entropy in thermally assisted reactions and considers only enthalpy. This is not always correct and can lead to unphysical conclusions.

In a thermally-activated reaction, the energy in the exponential term is actually the change in free energy, $\Delta F = \Delta H - T\Delta S$, where ΔH is the enthalpy change and ΔS the entropy change in the reaction. $E_a = \Delta H$ in this paper. The reaction rate is given by, $r_c = (kT/h)e^{-\Delta F/kT} = (kT/h)e^{-\Delta S/k}e^{-\Delta H/kT} = v_c e^{-\Delta H/kT}$ where k and h are the Boltzmann and Planck constants, respectively.[20] The last form is often used with the assumption that $\Delta S/k$ is small and can be neglected. The rate prefactor is then about 2×10^{10} T. Good examples of systems where ΔS should not be ignored are ones that obey the Meyer–Neldel or compensation rule.[21] In these cases ΔS is positive and proportional to ΔH so that the logarithm of the prefactor is proportional to the activation energy. A large number of physical systems obeying this rule have been found. Reference 21 contains a number of examples. One should decompose ΔS into a positive, $\Delta S_{mnr} = k\Delta H/T_{iso}$, and a negative term, ΔS_{con}.[22] Here, T_{iso} is the isokinetic temperature for systems that obey the Meyer–Neldel rule. The negative term is a configurational or barrier entropy change.[20] One can think of this configurational entropy as a measure of number of wrong configurations that are sampled until the right configuration is found. The "right configuration" is the one that allows the transition to go over the lowest energy barrier.[20] All the wrong configurations lead to much higher barriers. ΔS_{con} can be found from the $\Delta H = 0$ intercept of a Meyer–Neldel plot of $\ln(v_c)$ versus ΔH. Figure 6 is such a plot.

Steps (1) and (2) of dimer diffusion present an excellent example of an entropy barrier. The SQ to ST conversion, $O_2^{sq,++} \rightarrow O_2^{st,++}$, is the wrong conversion with the higher barrier, 0.86 eV.[1,2] The $O_2^{sq,+} \rightarrow O_2^{st,+}$ conversion has the lower, 0.17 eV, energy barrier.[1] Because the trapped electron is emitted so rapidly from the $O_2^{sq,++}$, most of the dimer vibrations probe the higher barrier. The data shown in Fig. 3 indicate that the lower barrier is found by experiment, as would be the case with an entropy barrier.

Another entropy barrier is presumably present in step (3) representing repulsive hole capture. Far from the defect, the potential is repulsive. Nevertheless the core presents an attractive potential.[23] Again the problem is finding the correct pathway. The Rose calculation is based on a continuum model assuming that at some close distance the repulsive potential is completely screened out.[18] In the real situation, there are directions of hole approach to the dimer where the potential is repulsive and some where it is attractive. Thus again there are many wrong paths and a few correct ones. This type of entropy barrier would contribute to the small prefactor for the lower temperature defect formation. Of course, defect formation also depends on hole and electron densities as well as the dimer and boron concentrations.[15] One can think of the entropy term as determining the capture rate coefficient in the thermally assisted hole capture step (3) in dimer diffusion.

The Meyer–Neldel plot in Fig. 6 includes data for formation as well as destruction of the BO_2 defect. Values from Ref. 24 differ from the general behavior observed by others. The authors[24] find a higher activation energy for formation than for annealing of the defects. Nevertheless the data lie along the line in Fig. 6. Defect formation was monitored by open-circuit voltage change. Recently, light-induced degradation of carrier lifetime was observed in n-type c-Si compensated with boron.[25] Annealing kinetics appear similar to those in uncompensated boron-doped material. However, the datum point lies considerably off the Meyer–Neldel line obtained for the p-type material.

It is not surprising that both degradation and annealing lie along the same Meyer–Neldel line because they use the same collective excitations to attain the thermal energy necessary to surmount energy barriers.[21] The slope of this line gives $T_{iso} = 410$ K, similar to values found for other crystalline semiconductors[21] but less than found recently by Trenhaile *et al.* for Br desorption on c-Si surface.[26]

The intercept of the line in Fig. 6 determines the entropy barrier to be $\Delta S_{con} = 37$ k. This barrier is most likely associated with step (2). It is not surprising that the low temperature degradation data scatter about this line since they depend strongly on the boron density as well as any entropy barrier. The high temperature degradation and annealing are determined by dimer diffusion and not hole capture. However, these variations should not obscure the fact that the dominant behavior of the system is determined by the entropy associated with thermal excitation. Any calculation of thermal rate prefactor should contain these entropy terms.

IV. CONCLUSIONS

The results of charge trapping measurements have yielded important new physics of the formation and destruction of the metastable defect in oxygen containing boron-doped crystalline silicon. The key finding of this work is that

an entropy barrier is encountered during the reaction $O_2^{sq,++} + e \rightarrow O_2^{st,+}$. This electron trapping reduces the normally 0.86 eV thermal activation barrier to 0.17 eV but at the expense of an abnormally low rate prefactor of 0.1 s^{-1}. The value of this entropy barrier is 37 k. At higher temperature this reaction dominates dimer diffusion. At low temperature this reaction is faster than the hole trapping reaction, $O_2^{st,+} + h \rightarrow O_2^{sq,++}$ so that the 0.4 eV repulse Coulomb capture can be observed. Annealing of the metastable defect results in the thermal emission of two holes with an activation energy of about 1.3 eV. Published defect annealing activation energies show considerable spread. Nevertheless they are consistent with a Meyer–Neldel rule behavior that relates the rate prefactor to the activation energy with an isokinetic temperature of 410 K.

ACKNOWLEDGMENTS

The author is indebted to Tihu Wang, Matthew Page, Hao-Chih Yuan, and David Young for sample preparation and other experimental help. I also benefited from many helpful discussions with Howard Branz and Mao-Hua Du. This work was supported by the U.S. Department of Energy under Contract No. DE-AC36-08-GO28308 with the National Renewable Energy Laboratory.

[1]M.-H. Du, H. M. Branz, R. S. Crandall, and S. B. Zhang, Phys. Rev. Lett. **97**, 256602 (2006).
[2]J. Adey, R. Jones, D. W. Palmer, P. R. Briddon, and S. Öberg, Phys. Rev. Lett. **93**, 055504 (2004).
[3]J. Schmidt, K. Bothe, and R. Hezel, *Proceedings of the 29th IEEE Photovoltaic Specialists Conference*, New Orleans, LA (IEEE, New York, 2002), p, 178.
[4]J. Schmidt and K. Bothe, Phys. Rev. B **69**, 024107 (2004).
[5]S. Rein, T. Rehl, W. Warta S. W.Glunz, and G. Willeke, *Proceedings of the 17th European Photovoltaic Solar Energy Conference*, Munich, Germany (WIP, Munich, 2001), p. 1555.
[6]S. W. Glunz, S. Rein, W. Warta, J. Knobloch, and W. Wettling, Sol. Energy Mater. Sol. Cells **65**, 219 (2001).
[7]J. Schmidt, K. Bothe, and R. Hezel, Appl. Phys. Lett. **80**, 4395 (2002).
[8]J. Schmidt and A. Cuevas, Appl. Phys. Lett. **86**, 3175 (1999).
[9]S. Rein, T. Rehrl, W. Warta, and S. W. Glunz, J. Appl. Phys. **91**, 2059 (2002).
[10]S. Rein and S. W. Glunz, Appl. Phys. Lett. **82**, 1054 (2003).
[11]H. Hashigami, M. Dhamrin, and T. Saitoh, Jpn. J. Appl. Phys., Part 1 **42**, 2564 (2003).
[12]H. Hashigami, Y. Itakura, and T. Saitoh, Sol. Energy Mater. Sol. Cells **75**, 351 (2003).
[13]K. Bothe, R. Hezel, and J. Schmidt, Appl. Phys. Lett. **83**, 1125 (2003).
[14]K. Bothe, R. Hezel, and J. Schmidt, Solid State Phenom. **95–96**, 223 (2004).
[15]D. W. Palmer, K. Bothe, and J. Schmidt, Phys. Rev. B **76**, 035210 (2007).
[16]R. S. Crandall, Phys. Rev. B **66**, 195210 (2002).
[17]T. H. Wang, E. Iwaniczko, M. R. Page, D. H. Levi, Y. Yan, H. M. Branz, and Q. Wang, Thin Solid Films **501**, 284 (2006).
[18]A. Rose, *Concepts in Photoconductivity and Allied Problems* (Interscience, New York, (1963).
[19]S. W. Johnston, private communication (July 2009).
[20]S. Glasstone, K. J. Laidler, and H. Eyring, *The Theory of Rate Processes* (McGraw-Hill, New York, 1941).
[21]A. Yelon, B. Movaghar, and R. S. Crandall, Rep. Prog. Phys. **69**, 1145 (2006).
[22]D. L. Young and R. S. Crandall, Appl. Phys. Lett. **86**, 262107 (2005).
[23]M.-H. Du, private communication (May 2008).
[24]T. K. Vu, Y. Oshita, K. Araki, and M. Yamaguchi, J. Appl. Phys. **91**, 4853 (2002).
[25]T. Schutz-Kuchly, J. Veirman, S. Dubois, and D. R. Heslinga, Appl. Phys. Lett. **96**, 093505 (2010).
[26]B. R. Trenhaile, V. N. Antonov, G. J. Xu, K. S. Nakayama, and J. H. Weaver, Surf. Sci. **583**, L135 (2005).